

Diamond Interchange Performance Measures Using Connected Vehicle Data

Enrique Saldivar-Carranza, Steven Rogers, Howell Li, Darcy Michael Bullock

Purdue University, West Lafayette, USA

Email: esaldiva@purdue.edu, roger239@purdue.edu, howell-li@purdue.edu, darcy@purdue.edu

How to cite this paper: Saldivar-Carranza, E., Rogers, S., Li, H. and Bullock, D.M. (2022) Diamond Interchange Performance Measures Using Connected Vehicle Data. *Journal of Transportation Technologies*, 12, 475-497. <https://doi.org/10.4236/jtts.2022.123029>

Received: June 1, 2022

Accepted: July 25, 2022

Published: July 28, 2022

Copyright © 2022 by author(s) and Scientific Research Publishing Inc.

This work is licensed under the Creative Commons Attribution International License (CC BY 4.0).

<http://creativecommons.org/licenses/by/4.0/>



Open Access

Abstract

Diamond interchanges are frequently used where a freeway intersects a two-way surface street. Most of the techniques to evaluate the performance of diamond interchanges rely on the Highway Capacity Manual (HCM), simulation, Automated Traffic Signal Performance Measures (ATSPMs), and historical crash data. HCM and simulation techniques require on-site data collection to obtain models' inputs. ATSPMs need high-resolution controller event data acquired from roadway sensing equipment. Safety studies typically need 3 to 5 years of crash data to provide statistically significant results. This study utilizes commercially available connected vehicle (CV) data to assess the performance and operation of a three- and four-phase diamond interchange located in Indianapolis, Indiana, and Dallas, Texas, respectively. Over 92,000 trajectories and 1,400,000 GPS points are analyzed from August 2020 weekdays CV data. Trajectories are linear-referenced to generate Purdue Probe Diagrams (PPDs) from which arrivals on green (AOG), split failures, downstream blockage, and movement-based control delay are estimated. In addition, an extension of the PPD is presented that characterizes the complete journey of a vehicle travelling through both signals of the diamond interchange. This enhanced PPD is a significant contribution as it provides an analytical framework and graphical summary of the operational characteristics of how the external movements traverse the entire system. The four-phase control showed high internal progression (99% AOG) compared to the moderate internal progression of the three-phase operation (64% AOG). This is consistent with the design objectives of three- and four-phase control models, but historically these quantitative AOG measures were not possible to obtain with just detector data. Additionally, a graphical summary that illustrates the spatial distribution of hard-braking and hard-acceleration events is also provided. The presented techniques can be used by any agency to evaluate the performance of their diamond interchanges without on-site data collection or capital investments in sensing infrastructure.

Keywords

Performance Measures, Safety, Connected Vehicle, Trajectories, Diamond Interchange

1. Introduction

Conventional diamond interchanges (CDI) transfer traffic between freeways and two-way surface streets [1]. Full CDIs consist of a pair of ramp intersections with relatively close interlocked left turns, four entry points, and four exit points [2] [3] [4] [5]. CDIs are crucial for the correct operation of urban transportation networks; hence, their safe and efficient operation are critical agency objectives [3] [4].

Currently, most performance evaluations of CDIs are done by means of Highway Capacity Manual (HCM) techniques or simulation. These model-based studies usually require intersection turning volumes to estimate vehicle delay, level of service (LOS) [6], number of stops, and queue-lengths [7]-[13]. Alternatively, a few studies have used high-resolution controller event data obtained from roadway sensing equipment to generate Automated Traffic Signal Performance Measures (ATSPMs) [2] [14] [15]. Safety performance has been assessed usually from three to five years of historical crash data [16] [17].

Connected vehicle (CV) trajectory, hard-braking (HB), and hard-acceleration (HA) data with nationwide coverage have recently become available from automotive manufacturers. These datasets provide opportunities for scalable and consistent infrastructure efficiency and safety assessments. CV trajectory data has been used to generate operational performance measures not only for conventional signalized intersections [18]-[23], but also for roundabouts [24] and diverging diamond interchanges (DDI) [25]. Additionally, HB events have been used as a surrogate for crash data [26] and HA events to assess driver behavior for different traffic signal phasing implementations [23]. However, no studies have used CV data to evaluate the performance of CDIs.

Due to the close proximity of the intersections on a diamond interchange, coordinating the ramp signals to manage the internal queues is critical to ensure they do not spill back and block upstream movements. To effectively manage a CDI, practitioners must evaluate the progression of vehicles traversing the interchange system and their effect on each approach [2]. Although there are design procedures for developing this signal phasing, variations in demand and driver behavior can significantly impact operations. Point-based detection used by ATSPMs makes it difficult to obtain accurate queue-length and movement-level performance measures.

With the recently available high-fidelity CV data, it is now possible to measure a sampling of vehicles' experience traversing a CDI on a movement-by-movement basis. This dataset has the capabilities of providing efficiency and safety performance measures without the need for on-site data collection, costly infrastruc-

ture investments, or long wait periods.

The objective of this study is to introduce methodologies based on CV data to measure arrivals on green (AOG), split failures (SF), downstream blockage (DSB), and movement-based control delay. Additionally, the distribution of HB and HA events is evaluated. This paper describes these techniques and discusses their application by analyzing operations at two diamond interchanges with three- and four-phase control.

1.1. Connected Vehicle Data

Indiana and Texas CV data for August 2020 weekdays, with an estimated penetration rate of 4.5% and 4.2% respectively [27], was used in this study. Two different CV datasets are utilized: trajectory data and event data.

1.1.1. CV Trajectory Data

The CV trajectory data consists of individual vehicle waypoints with latitude, longitude, the vehicle speed and heading, a timestamp, and an anonymized unique journey identifier. The data reports with a temporal frequency of three seconds and a spatial accuracy of 1.5 meters. For this study, over 92,000 unique journeys and 1.4 million waypoints are analyzed.

1.1.2. CV Event Data

The CV event data consists of individual HB and HA events, each of which has the following information attached: GPS location with a 1.5-meter fidelity radius, timestamp, speed, and heading. A HB event is recorded as soon as a vehicle's on-board accelerometer experiences an acceleration magnitude greater than 2.67 m/s^2 (as defined by the data provider). Likewise, HA has a 2.638 m/s^2 threshold to trigger the event.

2. Study Locations

To demonstrate the developed techniques for CDI assessment two different interchanges are evaluated. **Figure 1** shows the studied diamond interchange at I-465 and Michigan Rd. located in Indianapolis, Indiana. **Figure 2** shows the analyzed CDI at George Bush Turnpike and Preston Rd. located north of Dallas, Texas. The most relevant difference between these two locations for the purposes of this paper is the proximity of their intersections since it significantly affects operations. For the location in Indiana, the internal distance between stop bars is 500 ft. (152 m.). In contrast, the CDI in Texas has only 240 ft. (73 m.) of separation between the internal stop bars.

Each intersection at the CDIs has been marked as *X*, *Y*, *W*, and *Z* to facilitate reference throughout the paper.

3. Diamond Interchange Phasing

There are two main signal control techniques that are usually implemented at diamond interchanges: three-phase and four-phase [3] [5] [28]. Depending on



Figure 1. I-465 at Michigan Rd. in Indianapolis, Indiana (Map data: Google).



Figure 2. George Bush Tpke at Preston Rd. in Dallas, Texas (Map data: Google).

the chosen scheme, operations can significantly vary. The following subsections briefly describe each control's implementation.

3.1. Three-Phase Control

Three-phase control is commonly used at diamonds where the intersections are located more than 400 ft. (121 m.) apart [5]. Such is the case of the study location in Indiana (Figure 1), where the intersections are 500 ft. away from each

other. **Figure 3** illustrates the 3-phase control implemented at this location. **Figure 3(a)** shows a common representation of the phases on a simplified geometry diagram of the CDI. **Figure 3(b)** shows the ring structure for the left intersection (*X*) and **Figure 3(c)** shows the ring structure for the right intersection (*Y*).

The three phases are the entering arterial, the internal left turn, and the ramp movement at each signal. The distance between *X* and *Y* provides storage for ramp traffic. If no queue spillback occurs, three-phase operation usually generates less delay than four-phase control and facilitates two-way progression on the arterial when the offsets between the two signals are close to zero [5] [28].

3.2. Four-Phase Control

Four-phase control is typically used where interior left-turn volumes are high and the spacing between intersections is less than 400 ft. (122 m.) [5] [28]. Such is the case of the study location in Texas (**Figure 2**), where the intersections are 240 ft. apart. Although there are a variety of techniques that signal equipment vendors and state agencies use to implement four-phase control, we use the general ring diagram in **Figure 4**. **Figure 4(a)** shows a typical phase numbering scheme. **Figure 4(b)** shows the ring structure for the left intersections *W* (top ring) and *Z*

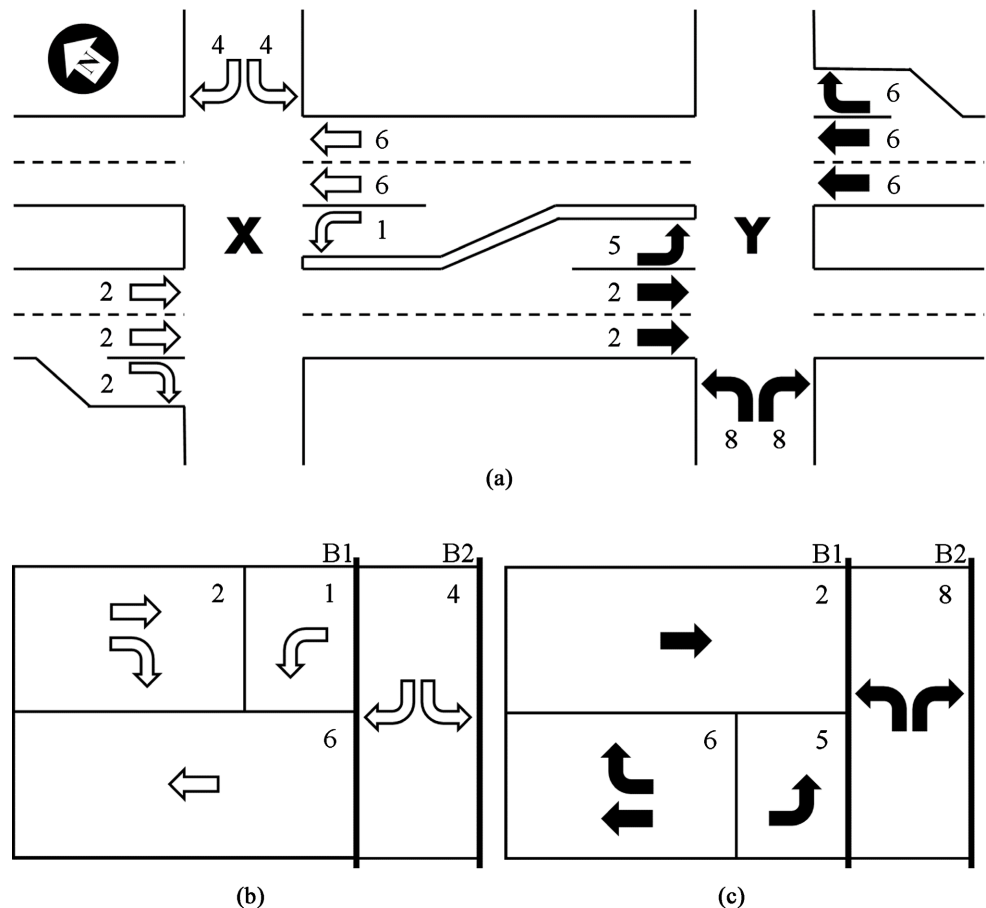


Figure 3. Three-phase diamond interchange phasing (Indiana). (a) Simplified geometry diagram; (b) *X* intersection ring structure; (c) *Y* intersection ring structure (B1 = barrier 1, B2 = barrier 2).

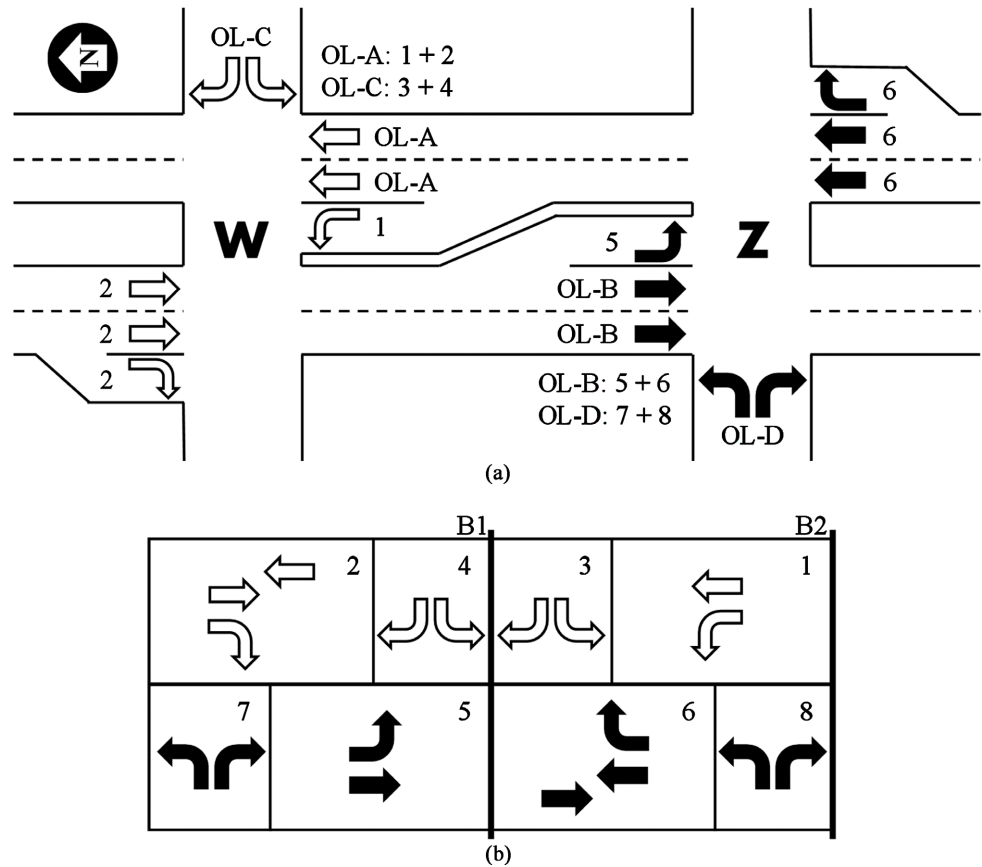


Figure 4. Four-phase diamond interchange phasing (Texas). (a) Simplified geometry diagram; (b) Ring structure (B1 = barrier 1, B2 = barrier 2, OL = overlap).

(bottom ring).

Both intersections of the interchange are tightly coordinated and are operated as if they were one big intersection. The four phases are the two arterial movements and the two ramp movements. If proper splits and offsets are set, this type of control provides progression through the interchange to all major movements which allows for an efficient queue management that is critical for CDIs with limited internal storage space [5] [28].

4. Diamond Interchange Performance Measures

In this section, the developed CV-based techniques for CDI assessment are discussed in the following order:

- 1) Standard Purdue Probe Diagrams (PPDs) for evaluating movements through one signal;
- 2) Extended PPDs for evaluating movement through both signals;
- 3) Internal and external movements performance summary by time-of-day;
- 4) Safety assessment from HA and HB events.

4.1. Purdue Probe Diagram

As the critical objective for CDI operation is to keep the internal storage free of

long queues to avoid spillback which blocks adjacent arterial and ramp movements, the progression of vehicles needs to be evaluated. The Purdue Probe Diagram [21] provides a systematic visualization of linear-referenced vehicles trajectories that pivot at the far side (FS) of the intersection. This provides a framework that allows for quantitative and qualitative approach-level analysis.

A PPD is a time-space diagram that color-codes vehicle trajectories based on the number of experienced stops, identified as horizontal lines, before crossing the FS of the intersection. The following performance measures can be estimated from PPDs:

- AOG: assessment of progression calculated as the proportion of non-stopping vehicles (color green).
- SF: indication of an approach operating on congested conditions calculated as the ratio of vehicles stopping more than once (color red or purple).
- DSB: measurement of the level of obstruction by adjacent intersections calculated as the ratio of vehicles slowing down or stopping after crossing the intersection.
- Control delay: summation of deceleration, stop, and acceleration delay. A free-flow trajectory (FFT) is also included in the PPD (black line) to facilitate qualitatively estimations of approach delay by comparing CV and FFT arrivals [21].

Figure 5 shows the PPDs of August 2020 weekdays vehicle trajectories that traversed the 3-phase CDI in Indiana from 16:00-18:00 hrs. **Figure 5(a)** shows the movements that conform the ring structure of intersection *X* (**Figure 3(b)**) ordered in the same manner. Only one movement is shown per phase, where exterior through movements have precedence followed by exterior left. Similarly, **Figure 5(b)** shows the movements that conform the ring structure of intersection *Y* (**Figure 3(c)**).

Figure 6 shows the PPDs of August 2020 weekdays vehicle trajectories that traversed the 4-phase CDI in Texas from 16:00-18:00 hrs. **Figure 6(a)** illustrates the movements that conform barrier 1 of the implemented ring structure (**Figure 4(b)**) and **Figure 6(b)** shows the movements that conform barrier 2.

The visualizations presented in this sub-section allow for a qualitative assessment of progression, congestion, queue-length, and delay at the movement level focused on the implemented signal control. For example, at the 3-phase CDI in Indiana, the southbound interior movements show a number of vehicles stopping once (**Figure 5(b)**, orange lines) at both the through (phase 2) and left turn (phase 5), while the northbound interior movements also show substantial arrivals on red. In contrast, the 4-phase CDI in Texas has internal through movements relatively well-progressed with all sampled vehicles having arrived on green southbound (OL-B) and a low density of one-stop trajectories in the northbound (OL-A). A limitation of the PPD is that each internal movement is shown in isolation and does not discern the origin of vehicles from the adjacent signal. This detail is important for assessing the quality of progression on the arterial.

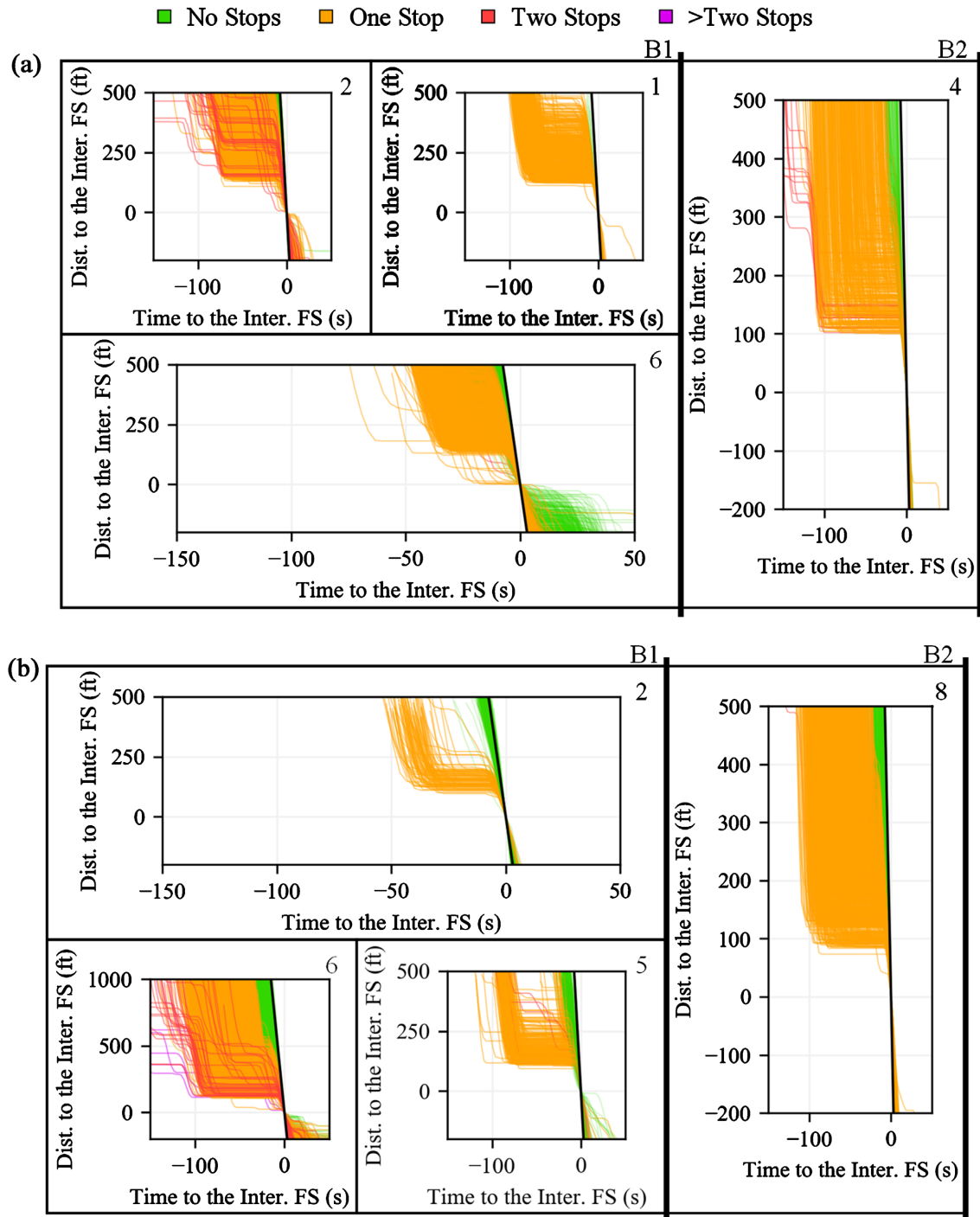


Figure 5. Purdue Probe Diagram for each movement in the ring structure of the 3-phase diamond in Indiana. (a) Intersection X ring structure; (b) Intersection Y ring structure (B1 = barrier 1, B2 = barrier 2, FS = far side).

4.2. Extended Purdue Probe Diagram

The Extended Purdue Probe Diagram (EPPD) is a visualization tool developed to show the queue and progression quality relative to a number of signals in a system to help assess performance based on the origin of vehicles.

EPPDs are based on the standard PPD (Figure 5 and Figure 6) [21], but instead

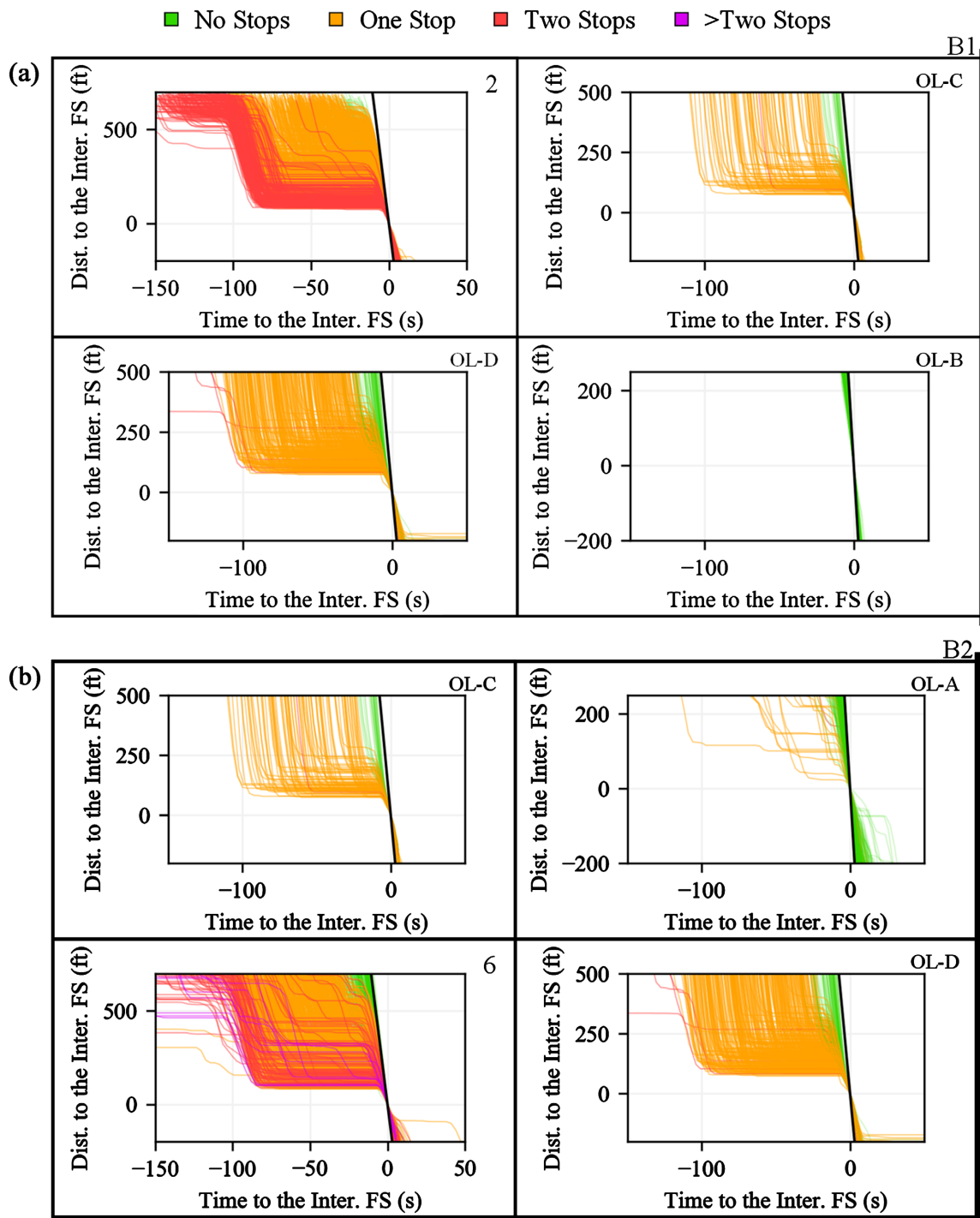


Figure 6. Purdue Probe Diagram for each movement in the ring structure of the 4-phase diamond in Texas. (a) Movements preceding barrier 1; (b) Movements preceding barrier 2 (B1 = barrier 1, B2 = barrier 2, FS = far side, OL = overlap).

of only characterizing the performance of a single signal approach, they show the complete movement of vehicles through a system of signals. This is accomplished by linear-referencing the distinct trips and pivoting at the last intersection’s far side of a complete origin-destination path. Each vehicle approach to

the different intersections is independently color-coded based on the number of stops. The trajectory's transition segment from one intersection to the next is shown in black. Additionally, the location of every signal's far side is indicated by horizontal lines for spatial referencing. Finally, a FFT is included to allow for delay estimations.

In the case of diamond interchanges only two intersections need to be included in the EPPD. The sampled volume distributions for the eight main origin-destination paths of the three- and four-phase controlled interchanges are provided on **Table 1** and **Table 2**, respectively. This information is relevant as it helps identify which paths have the highest demands and are more likely to congest the storage area.

Figure 7 shows the EPPDs of August 2020 weekdays vehicle trajectories that traversed the 3-phase CDI in Indiana from 16:00-18:00 hrs. The air photo in the lower left corner of all the figures have a movement arrow that graphically illustrates the path of vehicles analyzed in each EPPD. All EPPDs reveal significant number of vehicles stopping before entering the interchange and most of them show internal stops (callout i), except for **Figure 7(d)**. From this subfigure, it is apparent that the CDI is timed with the objective of serving and progressing vehicles coming off the westbound ramp to southbound as efficiently as possible, with essentially none of those vehicles having to stop internally at all. By looking at and connecting the trajectories across the two signals, the EPPD is able to shed light on decisions and safety trade-offs made in the signal timing plan.

Figure 8 shows EPPDs for six paths of August 2020 weekdays vehicle trajectories

Table 1. Sampled volume distribution at the 3-phase interchange in Indiana for August 2020 weekdays from 16:00 to 18:00 hrs.

Origin (external movements)	Destination (internal movements)			
	Y SB-Through	Y SB-Left	X NB-Through	X NB-Left
X SB-Through	14%	22%	-	-
X WB-Left	8%	0%	-	-
Y NB-Through	-	-	23%	11%
Y EB-Left	-	-	22%	0%

Table 2. Sampled volume distribution at the 4-phase interchange in Texas for August 2020 weekdays from 16:00 to 18:00 hrs.

Origin (external movements)	Destination (internal movements)			
	Z SB-Through	Z SB-Left	W NB-Through	W NB-Left
W SB-Through	21%	18%	-	-
W WB-Left	4%	0%	-	-
Z NB-Through	-	-	29%	15%
Z EB-Left	-	-	13%	1%

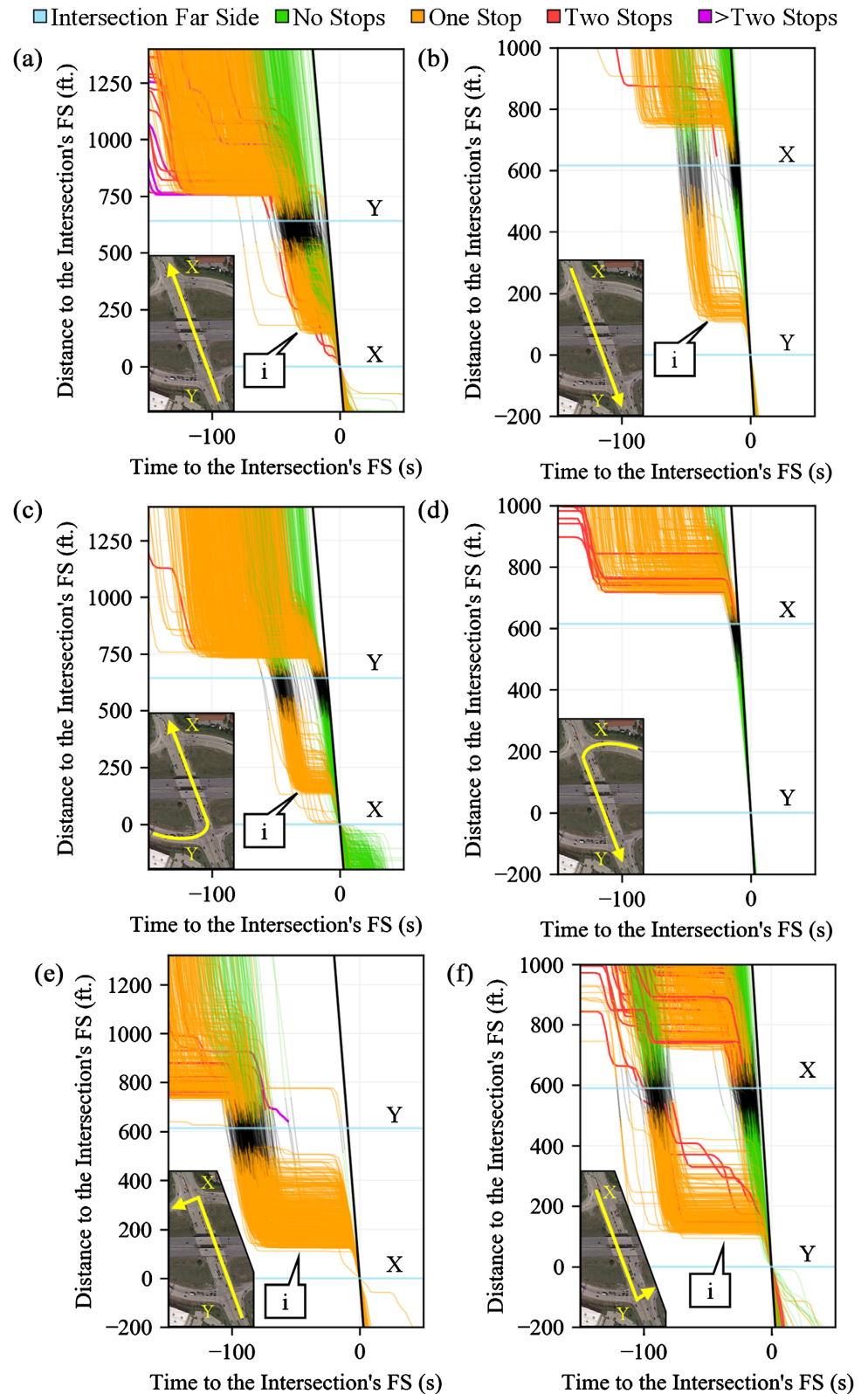


Figure 7. EPPDs for the 3-phase diamond in Indiana (Map data: Google). (a) NB-through at Y and NB-through at X; (b) SB-through at X and SB-through at Y; (c) EB-left at Y and NB-through at X; (d) WB-left at X and SB-through at Y; (e) NB-through at Y and NB-left at X; (f) SB-through at X and SB-left at Y (FS = far side).

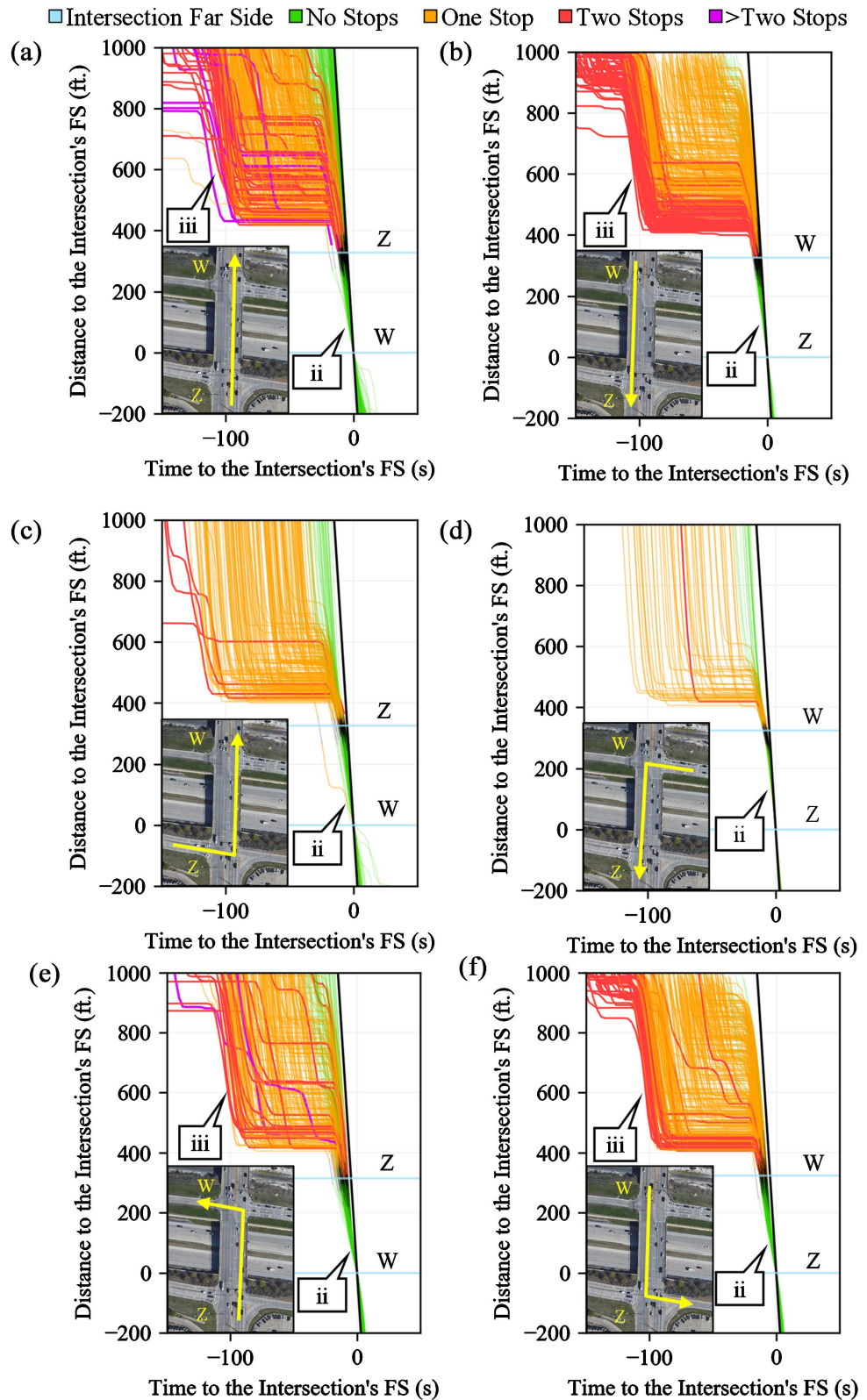


Figure 8. EPPDs for the 4-phase diamond in Texas (Map data: Google). (a) NB-through at Z and NB-through at W; (b) SB-through at W and SB-through at Z; (c) EB-left at Z and NB-through at W; (d) WB-left at W and SB-through at Z; (e) NB-through at Z and NB-left at W; (f) SB-through at W and SB-left at Z (FS = far side).

that traversed the four-phase CDI in Texas from 16:00-18:00 hrs. Similar to the interchange in Indiana, the CDI in Texas shows significant number of vehicles stopping before entering the system. However, once vehicles enter the interchange, they continue their progression unimpeded (callout ii), which is the main benefit of properly implemented four-phase control. This is an important characteristic as closely spaced intersections have higher risk of getting blocked by internal queues. The four-phase CDI operates similarly as a split-phased signal, which contributes to increased congestion on the movements entering the CDI (callout iii) shown by vehicles stopping more than once (color-coded red and purple).

The following subsection discusses performance evaluation by TOD.

4.3. Summary Performance by Time-of-Day

The EPPDs provide a detailed characterization of progression, stops, split failures, downstream blockage, and delay for a specific time period. However, it is important to have a comprehensive summarized overview of how all the movements perform across different time-of-day (TOD) periods to effectively evaluate a CDI. To address this need, graphical heat maps summarizing performance by movement and by TOD are proposed.

Figure 9 and **Figure 10** show heatmaps with 15-minute resolution indicating the percentage of vehicles arriving on green for the four external movements and four internal movements. For the three-phase controlled interchange (**Figure 9**), it is shown how the internal movements have AOG around 50% (callout iv),

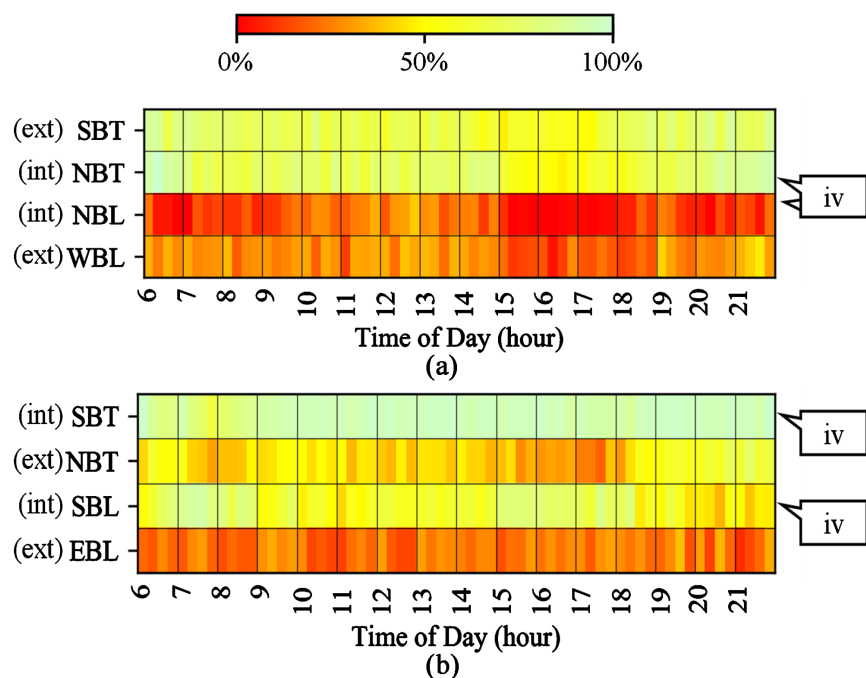


Figure 9. August 2020 weekdays arrivals on green by approach and movement for the 3-phase diamond interchange (Indiana). (a) Intersection X; (b) Intersection Y (ext = external, int = internal).

with northbound-left (NBL, **Figure 9(a)**) having poor progression (~0% AOG) and southbound-through (SBT, **Figure 9(b)**) having good progression (~100% AOG). For the four-phase controlled interchange (**Figure 10**), all internal movements have efficient progression as vehicles do not have to stop before exiting the CDI (callout v).

Figure 11 and **Figure 12** show the percentage of sampled vehicles that

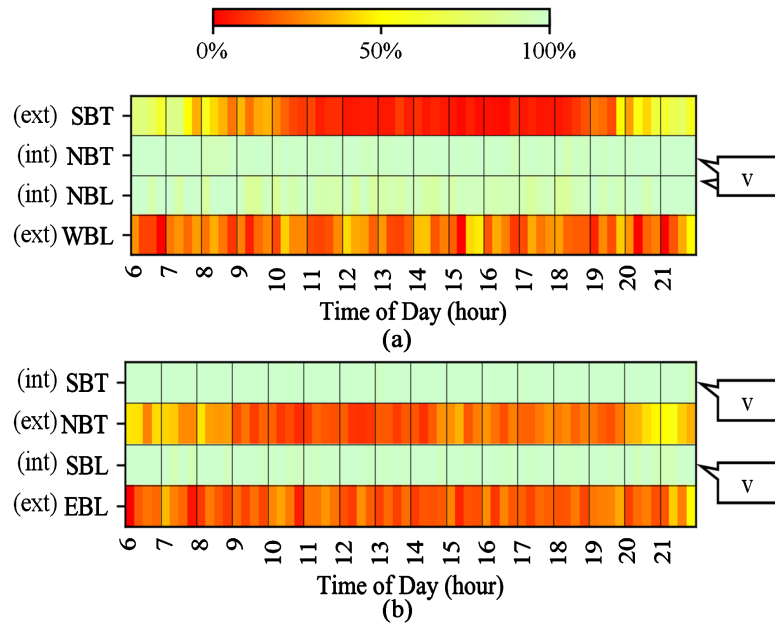


Figure 10. August 2020 weekdays arrivals on green by approach and movement for the 4-phase diamond interchange (Texas). (a) Intersection *W* (b) Intersection *Z*. (ext = external, int = internal).

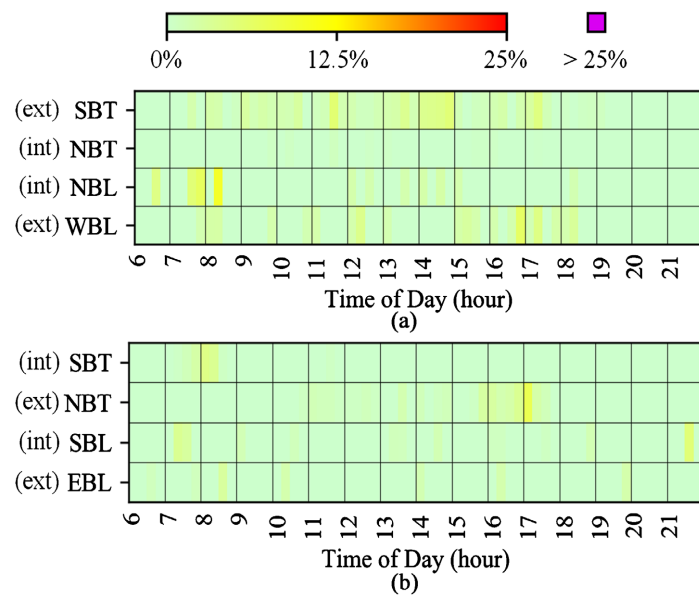


Figure 11. August 2020 weekdays split failures by approach and movement for the 3-phase diamond interchange (Indiana). (a) Intersection *X* (b) Intersection *Y*. (ext = external, int = internal).

experienced split failures at the three- and four-phase CDI intersections, by time of day. The three-phase control (Figure 11) has very few split failures throughout the day. The CDI shown in Figure 12 has significant split failures at most of the external movements during different TOD (callout vi) but no split failures on the internal movements.

Figure 13 and Figure 14 show heatmaps indicating the percentage of sampled vehicles that experienced DSB. For the CDI in Indiana (3-phase control, Figure 13),

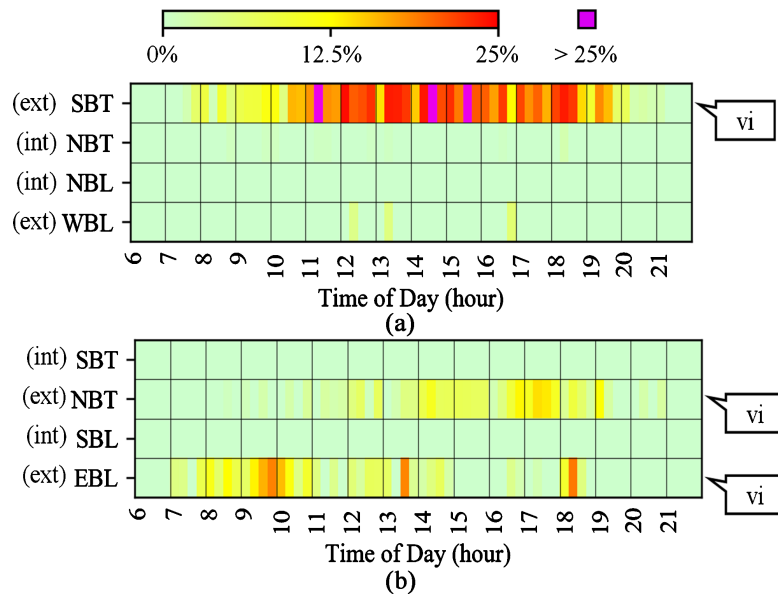


Figure 12. August 2020 weekdays split failures by approach and movement for the 4-phase diamond interchange (Texas). (a) Intersection W; (b) Intersection Z (ext = external, int = internal).

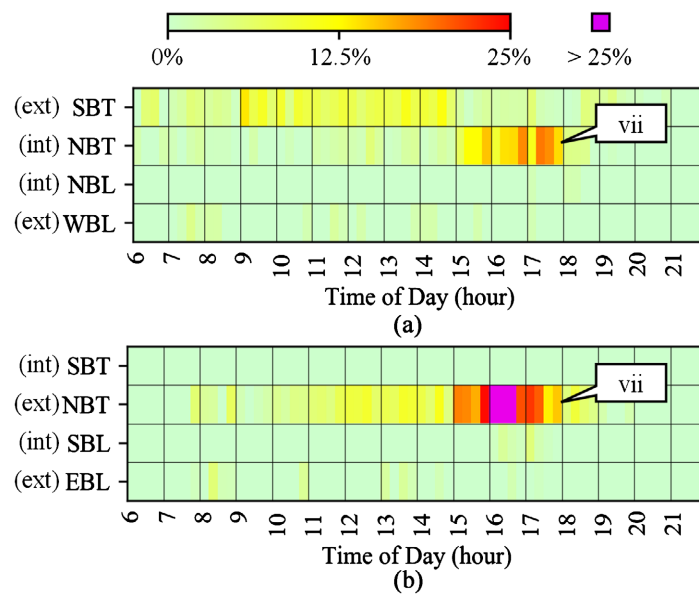


Figure 13. August 2020 weekdays downstream blockage by approach and movement for the 3-phase diamond interchange (Indiana). (a) Intersection X; (b) Intersection Y (ext = external, int = internal).

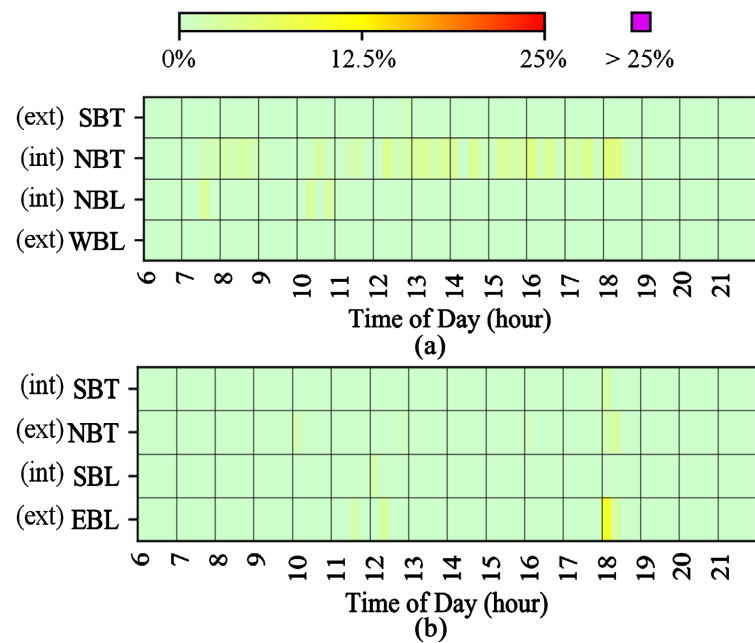


Figure 14. August 2020 weekdays downstream blockage by approach and movement for the 4-phase diamond interchange (Texas). (a) Intersection *W*; (b) Intersection *Z* (ext = external, int = internal).

the northbound-through (NBT) movements are being significantly obstructed soon after they cross each intersection during the PM peak period between 15:00 and 18:00 hrs. (callout vii). This is of particular interest as DSB is a consequence of long downstream queues. In the case of the external NBT movement (**Figure 13(b)**), this means that the internal CDI queue is long enough to affect progression. In contrast, four-phase control (**Figure 14**) has minimal number of vehicles experiencing DSB internally.

Finally, **Figure 15** and **Figure 16** show the LOS based on control delay (**Table 3**) for the relevant movements at the three- and four-phase CDI intersections, respectively. The effects that poor progression and congestion have on delay are illustrated.

The following subsection discusses the CV-event-based safety evaluation of CDIs.

4.4. Event-Based Safety Evaluation

Connected vehicle hard-acceleration and hard-braking events have proven to be effective datasets for the evaluation of safety at intersections without the need of long wait periods for statistically significant crash data [16] [17] [23] [26]. In this subsection, the HA and HB events patterns at the studied CDIs are evaluated.

Figure 17 and **Figure 18** show linear-referenced event histograms, pivoting at the stop bar of the entry intersection, color-coded based on the speed of the vehicle at the time of the event, for the three- and four-phase controlled interchanges, respectively. The event counts are normalized as a percentage of the number of unique CV trajectory identifiers sampled at the same location and

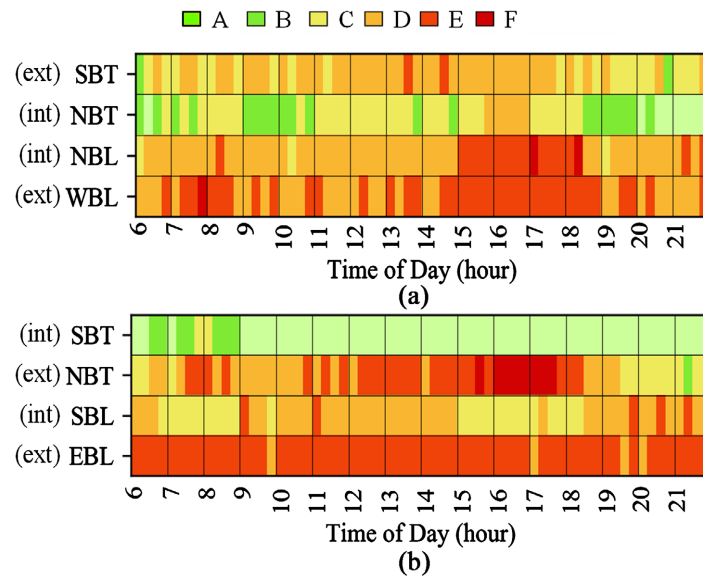


Figure 15. August 2020 weekdays HCM level of service by approach and movement for the 3-phase diamond interchange (Indiana). (a) Intersection *X*; (b) Intersection *Y* (ext = external, int = internal).

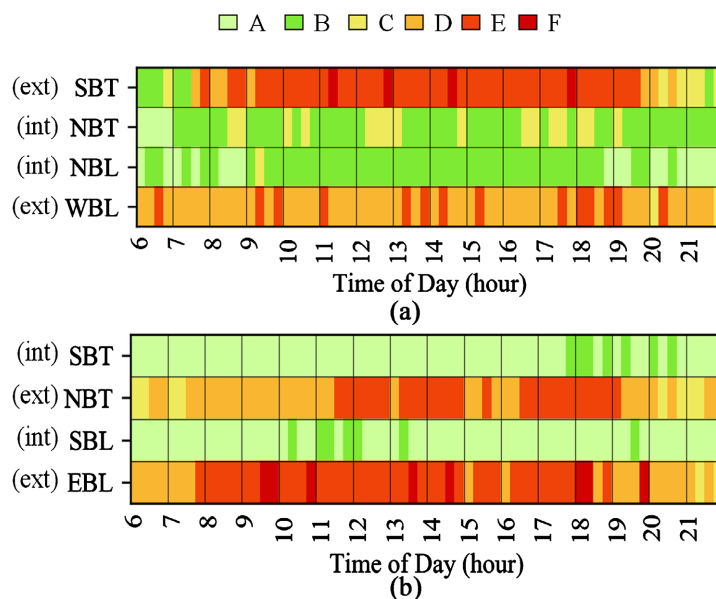


Figure 16. August 2020 weekdays HCM level of service by approach and movement for the 4-phase diamond interchange (Texas). (a) Intersection *W*; (b) Intersection *Z* (ext = external, int = internal).

time of the analysis.

Figure 17 shows results for vehicles traveling northbound-through at the Indiana interchange (three-phase signal control). Only a small percentage of sampled vehicles perform HB. In contrast, there are two significantly higher concentrations of HA (~1%) near the intersections’ stop bars (callout viii for *Y* and ix for *X*) made up mainly from slow-speed traveling vehicles (0 - 20 mph). This may be an indication of drivers rushing through the intersection as soon as they

Table 3. HCM level of service criteria for signalized intersection [6].

Level of Service	Average Control Delay (sec/vehicle)	Description
A	≤10	Free Flow
B	>10 - 20	Stable Flow (slight delay)
C	>20 - 35	Stable Flow (acceptable delays)
D	>35 - 55	Approaching Unstable Flow (tolerable delay)
E	>55 - 80	Unstable Flow (intolerable delay)
F	>80	Forced Flow (congested and queues fail to clear)

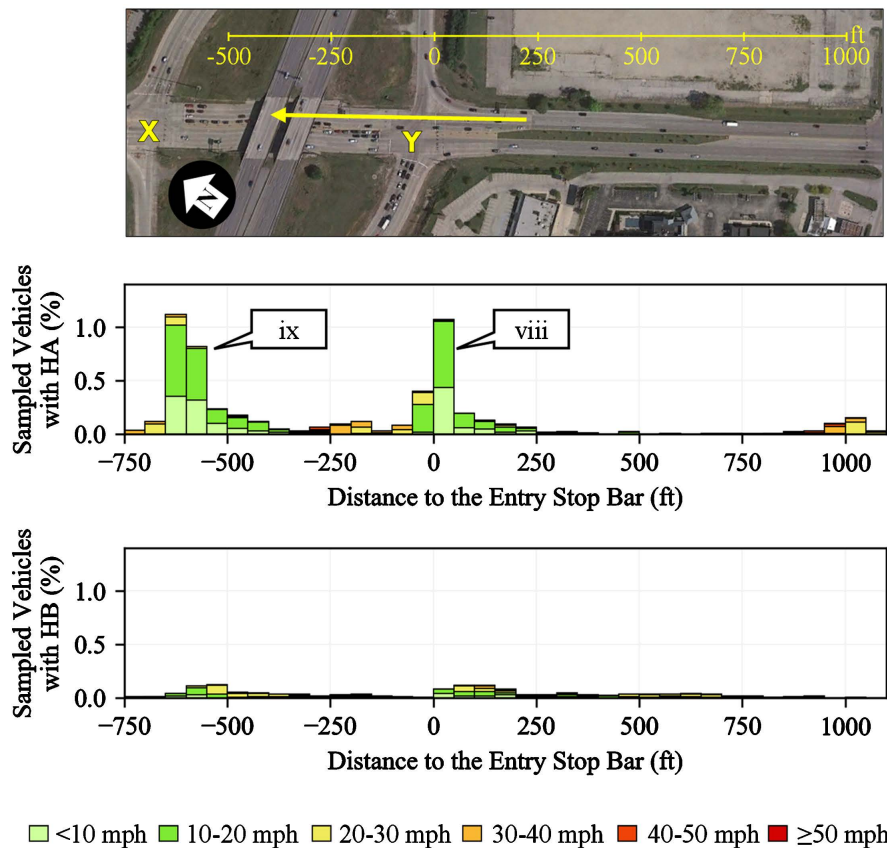


Figure 17. August 2020 weekdays normalized HA and HB CV events of vehicles traveling NB through on the 3-phase diamond interchange in Indiana.

are given green or vehicles traveling with a moving queue attempting to clear the intersection before the onset of amber.

Figure 18 shows results for vehicles traveling southbound-through at the Texas CDI (four-phase signal control). Similar to the Indiana interchange, just a small percentage of sampled vehicles have HB. However, the Texas CDI only presents one concentration of HA events near the entry intersection’s stop bar (callout x for *W*). As progression at the exit intersection (*Z*) is highly efficient (~100% AOG, **Figure 10(b)**), drivers do not have to rush to cross; hence, the

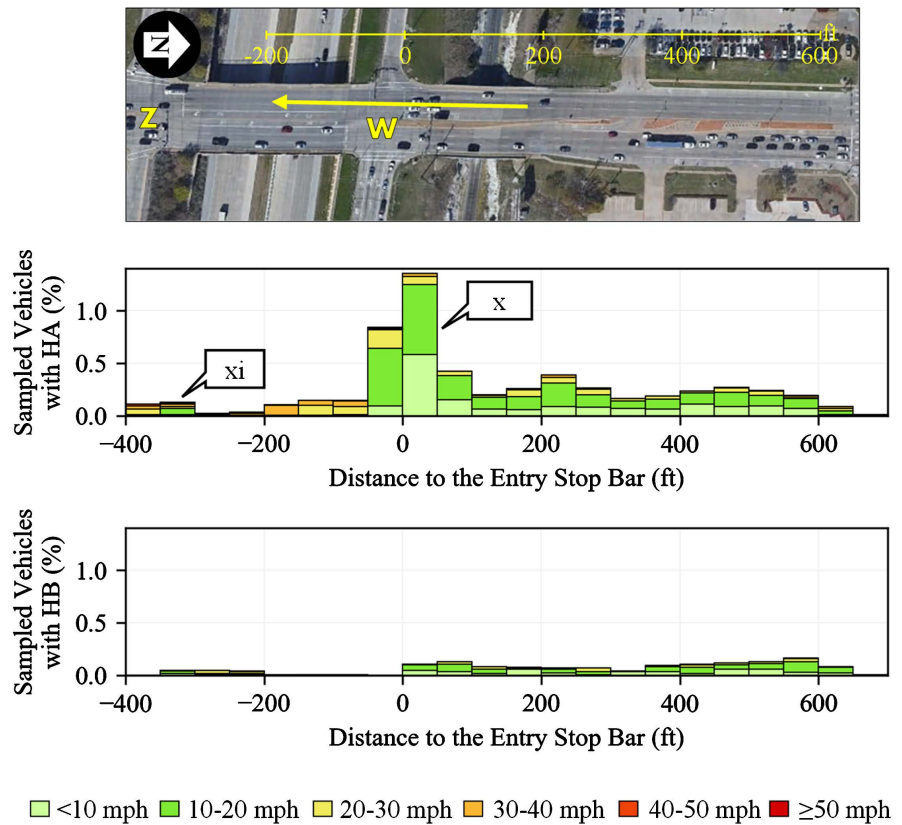


Figure 18. August 2020 weekdays normalized HA and HB CV events of vehicles traveling SB through on the 4-phase diamond interchange in Texas.

proportion of vehicles hard-accelerating is smaller (callout xi).

5. Results and Discussion

Table 4 shows a summary of the evaluated efficiency-oriented performance measures for the PM peak period (16:00-18:00 hrs.). Although these intersections have different demand volumes and configuration, it is interesting to compare their operation as they provide a good comparison of the tradeoffs between three- and four-phase control. Trajectory data for the four-phase CDI demonstrated high internal progression (99% AOG), as is intended by its signal control. In contrast, the three-phase control showed only moderate internal progression (64% AOG). In regard to downstream blockage, the operation of the four-phase signal resulted in 1% of internal DSB despite over-saturated external movements that had approximately 11% split failures. The three-phase control had substantially higher internal downstream blockage (7%), despite having a much smaller number of split failures on the exterior movements (2%).

Comparing two different interchanges with different contexts and volumes is not a common engineering practice; however, it provides a framework on how to evaluate CDIs to select three- or four-phase operation from objective data. This can be particularly useful for agencies to determine the type of control to use where the intersections at an interchange are close to the 400 ft. threshold.

Table 4. Timing implementation PM peak (16:00-18:00 hrs.) performance comparison.

Performance Measure	Three-phase Control	Four-phase Control
Internal Movements AOG	64%	99%
Internal Movements SF	0%	0%
Internal Movements DSB	7%	1%
External Movements AOG	38%	16%
External Movements SF	2%	11%
External Movements DSB	8%	0%

The ability to have performance measures such as those shown in **Table 4**, provide quantitative information for an agency to tune their time-of-day schedule to identify what hours of the day a diamond interchange must be operated in four-phase to avoid internal congestion, and what hours of the day the diamond interchange can operate in a more efficient three-phase operation.

6. Conclusions

This study presented techniques based on commercially available connected vehicle trajectory and event data to assess the efficiency and safety performance of conventional diamond interchanges. To demonstrate the methodologies, performance measures at a three- and four-phase signal-controlled CDIs were calculated. Over 92,000 trajectories and 1,400,000 GPS points were processed from August 2020 weekday CV data to generate the following:

- Ring-structure-oriented PPD (**Figure 5** and **Figure 6**): A PPD configuration that provides insight on the approach-level performance of the relevant movements of the implemented ring structure.
- Extended Purdue Probe Diagram (**Figure 7** and **Figure 8**): Variation of the PPD that shows the complete progression of vehicles traversing entire signal systems. This visualization is particularly relevant for CDI evaluation since it allows for a holistic view of origin-destination dynamics to support or reinforce signal timing objectives.
- Arrivals on green, split failures, downstream blockage, and level of service heat map summaries by TOD that show results for the critical internal and external movements at each intersection (**Figure 9** to **Figure 16**).
- Evaluation of the distribution of hard-acceleration and hard-braking events (**Figure 17** and **Figure 18**).

The presented techniques for diamond interchange evaluation can be used anywhere in the world where CV data is available without the need of on-site data collection, significant capital investment, or long wait periods.

Acknowledgements

Connected vehicle trajectory and event data for August 2020 weekdays used in this study was provided by Wejo Data Services, Inc. This work was supported in

part by the Joint Transportation Research Program and Pooled Fund Study (TPF-5(377)) led by the Indiana Department of Transportation (INDOT) and supported by the state transportation agencies of California, Connecticut, Georgia, Minnesota, North Carolina, Ohio, Pennsylvania, Texas, Utah, Wisconsin, plus the City of College Station, Texas, and the FHWA Operations Technical Services Team. The contents of this paper reflect the views of the authors, who are responsible for the facts and the accuracy of the data presented herein, and do not necessarily reflect the official views or policies of the sponsoring organizations. These contents do not constitute a standard, specification, or regulation.

Conflicts of Interest

The authors declare no conflicts of interest regarding the publication of this paper.

References

- [1] Chang, M.S. and Messer, C.J. (1985) Volume Guidelines for Signalization of Diamond Interchanges. *Transportation Research Record: Journal of the Transportation Research Board*, **1010**, 29-37.
- [2] Hainen, A.M., Li, H., Stevens, A.L., Day, C.M., Sturdevant, J.R. and Bullock, D.M. (2015) Sequence Optimization at Signalized Diamond Interchanges Using High-Resolution Event-Based Data. *Transportation Research Record: Journal of the Transportation Research Board*, **2487**, 15-30. <https://doi.org/10.3141/2487-02>
- [3] Messer, C.J. and Chang, M.S. (1987) Traffic Operations of Basic Traffic-Actuated Control Systems at Diamond Interchanges. *Transportation Research Record*, **1114**, 54-62.
- [4] Messer, C.J. and Chang, M.S. (1985) Traffic Operations of Basic Actuated Traffic Control Systems at Diamond Interchanges. Research Report 344-2F. Texas State Department of Highways and Public Transportation, Austin.
- [5] Venglar, S., Koonce, P. and Urbanik II, T. (1998) Passer III-98 Application and User's Guide. Texas Transportation Institute, College Station.
- [6] Transportation Research Board (TRB) (2010) Highway Capacity Manual 2010. National Research Council (NRC), Washington DC.
- [7] Chlewicki, G. (2003) New Interchange and Intersection Designs: The Synchronized Split-Phasing Intersection and the Diverging Diamond Interchange. *2nd Urban Street Symposium: Uptown, Downtown, or Small Town: Designing Urban Streets That Work*, Anaheim, 28-30 July 2003, 16 p.
- [8] Khan, T. and Anderson, M. (2016) Evaluating the Application of Diverging Diamond Interchange in Athens, Alabama. *International Journal for Traffic and Transport Engineering*, **6**, 38-50. [https://doi.org/10.7708/ijtte.2016.6\(1\).04](https://doi.org/10.7708/ijtte.2016.6(1).04)
- [9] Tarko, A.P., Romero, M.A. and Sultana, A. (2017) Performance of Alternative Diamond Interchange Forms: Volume 2—Guidelines for Selecting Alternative Diamond Interchanges. Joint Transportation Research Program Publication No. FHWA/IN/JTRP-2017/02, Purdue University, West Lafayette. <https://doi.org/10.5703/1288284316386>
- [10] Lee, S., Lee, C. and Kim, D.G. (2014) Design and Evaluation of Actuated Four-Phase Signal Control at Diamond Interchanges. *KSCE Journal of Civil Engineering*, **18**, 1150-1159. <https://doi.org/10.1007/s12205-014-0499-x>

- [11] Jones, S.L., Sullivan, A., Anderson, M., Malave, D. and Cheekoti, N. (2004) Traffic Simulation Software Comparison Study. UTCA Report 02217.
- [12] Lee, S., Messer, C.J., Oh, Y. and Lee, C. (2004) Assessment of Three Simulation Models for Diamond Interchange Analysis. *Journal of Transportation Engineering*, **130**, 304-312. [https://doi.org/10.1061/\(ASCE\)0733-947X\(2004\)130:3\(304\)](https://doi.org/10.1061/(ASCE)0733-947X(2004)130:3(304))
- [13] Xu, H., Liu, H. and Tian, Z. (2010) Control Delay at Signalized Diamond Interchanges Considering Internal Queue Spillback. *Transportation Research Record: Journal of the Transportation Research Board*, **2173**, 123-132. <https://doi.org/10.3141/2173-15>
- [14] Hainen, A.M., Stevens, A.L., Freije, R.S., Day, C.M., Sturdevant, J.R. and Bullock, D.M. (2014) High-Resolution Event-Based Data at Diamond Interchanges: Performance Measures and Optimization of Ring Displacement. *Transportation Research Record: Journal of the Transportation Research Board*, **2439**, 12-26. <https://doi.org/10.3141/2439-02>
- [15] Day, C.M., Bullock, D.M., Li, H., *et al.* (2014) Performance Measures for Traffic Signal Systems: An Outcome-Oriented Approach. Purdue University, West Lafayette. <https://doi.org/10.5703/1288284315333>
- [16] Roupail, N.M. and Hummer, J.E. (2014) Field Evaluation of Diverging Diamond Interchanges. TechBrief.
- [17] Claros, B.R., Edara, P., Sun, C. and Brown, H. (2015) Safety Evaluation of Diverging Diamond Interchanges in Missouri. *Journal of the Transportation Research Board*, **2486**, 1-10. <https://doi.org/10.3141/2486-01>
- [18] Zhao, Y., Zheng, J., Wong, W., Wang, X., Meng, Y. and Liu, H.X. (2019) Estimation of Queue Lengths, Probe Vehicle Penetration Rates, and Traffic Volumes at Signalized Intersections using Probe Vehicle Trajectories. *Transportation Research Record: Journal of the Transportation Research Board*, **2673**, 660-670. <https://doi.org/10.1177/0361198119856340>
- [19] Cetin, M. (2012) Estimating Queue Dynamics at Signalized Intersections from Probe Vehicle Data: Methodology Based on Kinematic Wave Model. *Transportation Research Record: Journal of the Transportation Research Board*, **2315**, 164-172. <https://doi.org/10.3141/2315-17>
- [20] Waddell, J.M., Remias, S.M. and Kirsch, J.N. (2020) Characterizing Traffic-Signal Performance and Corridor Reliability Using Crowd-Sourced Probe Vehicle Trajectories. *Journal of Transportation Engineering, Part A: Systems*, **146**, Article ID: 04020053. <https://doi.org/10.1061/JTEPBS.0000378>
- [21] Saldivar-Carranza, E.D., Li, H., Mathew, J.K., Hunter, M., Sturdevant, J. and Bullock, D.M. (2021) Deriving Operational Traffic Signal Performance Measures from Vehicle Trajectory Data. *Transportation Research Record: Journal of the Transportation Research Board*, **2675**, 1250-1264. <https://doi.org/10.1177/03611981211006725>
- [22] Saldivar-Carranza, E.D., Hunter, M., Li, H., Mathew, J.K. and Bullock, D.M. (2021) Longitudinal Performance Assessment of Traffic Signal System Impacted by Long-Term Interstate Construction Diversion Using Connected Vehicle Data. *Journal of Transportation Technologies*, **11**, 644-659. <https://doi.org/10.4236/jtts.2021.114040>
- [23] Saldivar-Carranza, E.D., Mathew, J.K., Li, H., Hunter, M., Platte, T. and Bullock, D.M. (2021) Using Connected Vehicle Data to Evaluate Traffic Signal Performance and Driver Behavior after Changing Left-turns Phasing. 2021 *IEEE International Intelligent Transportation Systems Conference (ITSC)*, Indianapolis, 19-22 September 2021, 4028-4034. <https://doi.org/10.1109/ITSC48978.2021.9564654>

-
- [24] Saldivar-Carranza, E.D., Mathew, J.K., Li, H. and Bullock, D.M. (2022) Roundabout Performance Analysis Using Connected Vehicle Data. *Journal of Transportation Technologies*, **12**, 42-58. <https://doi.org/10.4236/jtts.2022.121003>
- [25] Saldivar-Carranza, E.D., Li, H. and Bullock, D.M. (2021) Diverging Diamond Interchange Performance Measures Using Connected Vehicle Data. *Journal of Transportation Technologies*, **11**, 628-643. <https://doi.org/10.4236/jtts.2021.114039>
- [26] Hunter, M., Saldivar-Carranza, E., Desai, J., Mathew, J., Li, H. and Bullock, D.M. (2021) A Proactive Approach to Evaluating Intersection Safety Using Hard-Braking Data. *Journal of Big Data Analytics in Transportation*, **3**, 81-94. <https://doi.org/10.1007/s42421-021-00039-y>
- [27] Hunter, M., Mathew, J.K., Li, H. and Bullock, D.M. (2021) Estimation of Connected Vehicle Penetration on US Roads in Indiana, Ohio, and Pennsylvania. *Journal of Transportation Technologies*, **11**, 597-610. <https://doi.org/10.4236/jtts.2021.114037>
- [28] Nelson, E.J., Bullock, D. and Urbanik, T. (2000) Implementing Actuated Control of Diamond Interchanges. *Journal of Transportation Engineering*, **126**, 390-395. [https://doi.org/10.1061/\(ASCE\)0733-947X\(2000\)126:5\(390\)](https://doi.org/10.1061/(ASCE)0733-947X(2000)126:5(390))